Analysis and Optimization of Pressure Retarded Osmosis for Power Generation

Mingheng Li
Dept. of Chemical and Materials Engineering, California State Polytechnic University, Pomona, CA 91768

DOI 10.1002/aic.14715
Published online January 6, 2015 in Wiley Online Library (wileyonlinelibrary.com)

Model-based analysis and optimization of pressure retarded osmosis (PRO) for power generation is focused. The effects of membrane properties (hydraulic permeability and mass-transfer characteristics), design conditions (inlet osmotic pressures, inlet flows, and membrane area) and operating condition (applied pressure) on power density and efficiency are systematically investigated. A dimensionless design parameter $\gamma = AL_p\pi_0^D/Q_0$, originally developed in analysis and optimization of reverse osmosis, is used to quantify the effect of dilution in draw solution (DS) as water permeates through membrane. An optimization method is developed to maximize PRO performance. It is shown that dilution and concentration polarization significantly reduce the maximum power density, and the optimal ΔP shifts away from $\Delta\pi_0/2$. Moreover, power density and efficiency follow opposite trends when varying process conditions including DS flow rate and membrane area. Enhancing membrane properties is crucial to improve the economic feasibility of PRO.
 AIChE J, 61: 1233–1241, 2015
Keywords: pressure retarded osmosis, power density, power efficiency, concentration polarization, optimization

Introduction

Pressure Retarded Osmosis (PRO) is a process to retrieve energy from the difference in salt concentrations between two solutions using a semipermeable membrane.[1] When a low-salinity feed solution (FS) and a pressurized high-salinity draw solution (DS) are separated by a membrane, water permeates from the FS into the DS, and the gained hydraulic energy in the DS may be harvested by a hydroturbine. The most common PRO process pairs river water and seawater.[2,3] Based on an assumed 40% energy conversion efficiency in PRO, the surface runoff of landwater to ocean in the United States has a potential to generate 55 GW electricity.[4] Interested readers are referred to excellent review papers[4–6] and references therein for the history, current development and perspective of this technology.

While PRO is acknowledged as a promising clean energy technology,[7–10] research and development efforts are still needed to improve its power density, efficiency, and economic feasibility. For example, concentration polarization adversely affects flux and power production, and extensive experimental studies have been conducted to investigate this phenomenon.[9,11–14] The experimental investigations are accompanied by modeling efforts to study transport phenomena[15–17] and thermodynamics[18,19] involved in PRO and to shed insight into the improvement of this process.

In modeling of PRO, constant transmembrane hydraulic and osmotic pressures (or averaged pressures) are commonly assumed. The water flux across membrane, J_w, is calculated by[14]

$$J_w = L_p(\Delta\pi - \Delta P) \tag{1}$$

where L_p is membrane hydraulic permeability, ΔP and $\Delta\pi$ are the transmembrane hydraulic and osmotic pressures, respectively. The hydraulic power available is[4,14]

$$W = Q_w\Delta P = AL_p(\Delta\pi - \Delta P)\Delta P \tag{2}$$

where Q_w is water flow rate across membrane and A is membrane area. The maximum of hydraulic power is $AL_p(\Delta\pi)^2/4$, and the corresponding optimal ΔP is $\Delta P_{opt} = \Delta\pi/2$.[4,14]

However, it should be noted that the above conclusion may be inaccurate when $\Delta\pi$ is not a constant. As water flows across a membrane (e.g., in a spiral wound module), the DS is diluted and its osmotic pressure decreases longitudinally.[8,11,20] The reduction in osmotic pressure may be significant if the dilution ratio is large. In this case, J_w reduces along the membrane channel, and Q_w should be calculated by $\int_0^A J_w dA$. When Eq. 2 is used to calculate hydraulic power, $\Delta\pi$ is better replaced by an averaged parameter $\overline{\Delta\pi}$, or

$$W = Q_w\Delta P = AL_p(\overline{\Delta\pi} - \Delta P)\Delta P \tag{3}$$

From optimization theory, $\Delta P_{opt} = \overline{\Delta\pi}/2$ is valid only if $\overline{\Delta\pi}$ is independent of ΔP. As will be shown later, $\overline{\Delta\pi}$ may be a function of ΔP.

This article focuses on system-level analysis and optimization of power generation in PRO. Using mathematical models, it is possible to provide an unambiguous understanding of the coupled behavior among various membrane and

Correspondence concerning this article should be addressed to M. Li at minghengli@cpp.edu.

process parameters and how they would affect power density and efficiency. In this computational work, concentration polarization is first ignored to clearly show the effect of dilution, and then included in a more comprehensive model.

Results and Discussion

Analysis ignoring concentration polarization

In the following analysis, it is assumed that the change in the FS osmotic pressure along the membrane channel is negligible as compared to that of the DS. This assumption is justified if the salinity of FS is much lower than the one of DS, or the flow rate of FS is much larger than the one of DS. It is further assumed that salt leakage across membrane is negligible. Moreover, the pressure drop in both FS and DS channels are not considered in this work. These simplifications are made so that the effect of several key process parameters on PRO performance can be revealed. A comprehensive model accounting for all transport phenomena would require coupling of more equations which can be handled by commercial computational tools, for example, COMSOL Multiphysics.[21]

Consider such a PRO process using spiral wound membranes, water flow rate across a membrane area of dA ignoring concentration polarization is given by

$$\frac{dQ}{dA} = L_p(\Delta\pi - \Delta P) = L_p\left(\pi_0^D \frac{Q_0}{Q} - \pi_0^F - \Delta P\right) \tag{4}$$

where dQ is water flow across membrane area dA. Q is DS flow rate. Subscript 0 represents properties at inlet. Superscript D and F represent DS and FS, respectively.

With definitions of dimensionless parameters $\theta = (\Delta P + \pi_0^F)/\pi_0^D$, $q = Q/Q_0$, and $\gamma = AL_p\pi_0^D/Q_0$, Eq. 4 is converted to a compact form as follows

$$\frac{dq}{dx} = \gamma\left(\frac{1}{q} - \theta\right) \tag{5}$$

where x is a dimensionless number from 0 to 1 ($dA = Adx$). Using the method of separation of variables, Eq. 5 may be rearranged and integrated from inlet to outlet of the membrane

$$\int_1^{q_d} \frac{q}{1-q\theta} dq = \int_0^1 \gamma dx \tag{6}$$

or

$$\gamma = \frac{1}{\theta}\left[1 - q_d + \frac{1}{\theta}\ln\frac{1-\theta}{1-q_d\theta}\right] \tag{7}$$

where q_d is the dilution ratio, or the DS flow rate at the membrane outlet divided by the one at the inlet. Water flow rate across the membrane is $Q_w = \int_0^A J_w dA = (q_d - 1)Q_0$.

It is worth pointing out that Eq. 7 is in the same form as the one derived for reverse osmosis (RO),[22,23] except that the range of q_d is different ($q_d > 1$ in PRO while $0 < q_d < 1$ in RO). Equation 7 is a characteristic equation of PRO that reveals the coupled behavior among design parameter γ, operation parameter θ, and performance parameter q_d. Knowing two parameters would determine the remaining one. Equation 7 is solved numerically using different values of γ (0.5–10) and θ (0.05–0.95) and the result is shown in Figure 1. It is clearly seen that the dilution ratio q_d increases as γ increases or θ decreases.

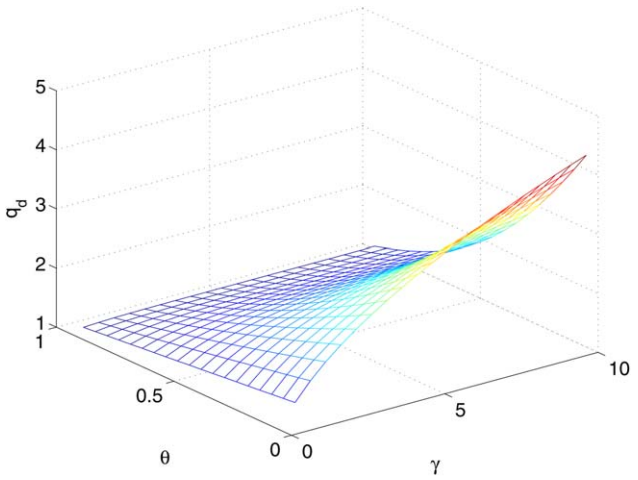

Figure 1. Contour of q_d in PRO as a function of γ and θ.

[Color figure can be viewed in the online issue, which is available at wileyonlinelibrary.com.]

Following the definition of specific energy consumption (SEC) in RO, specific energy production (SEP) in PRO may be defined as the theoretical hydraulic power per unit DS inlet flow rate. SEP ignoring the effect of hydraulic turbine efficiency has the following form

$$\text{SEP} = \frac{Q_0(q_d - 1)\Delta P}{Q_0} = (q_d - 1)\Delta P \tag{8}$$

The SEP normalized by the DS inlet osmotic pressure, or normalized specific energy production (NSEP), is a dimensionless number

$$\text{NSEP} = \frac{\text{SEP}}{\pi_0} = (q_d - 1)(\theta - r) \tag{9}$$

where r is the inlet osmotic pressure ratio ($r = \pi_0^F/\pi_0^D$). Because $\text{NSEP} = W/(Q_0\pi_0^D)$, it may also be interpreted as the conversion efficiency from osmotic energy to hydraulic energy (η_{O2H}) for a salinity stream in PRO, that is

$$\eta_{O2H} = \text{NSEP} \tag{10}$$

The relationship between power density (PD, in the unit of W/m^2)[9,24] and NSEP is

$$\text{PD} = (\text{NSEP})(Q_0/A)\pi_0^D = (\text{NSEP})L_p(\pi_0^D)^2/\gamma \tag{11}$$

When Q_0/A and π_0^D are fixed, PD and NSEP (or η_{O2H}) are proportional, that is, to maximize PD and to maximize NSEP are equivalent.

The relationship between θ and $\Delta P/\Delta\pi_0$ is described by the following

$$\frac{\Delta P}{\Delta\pi_0} = \frac{\theta - r}{1 - r} \tag{12}$$

If $r = 0$ (e.g., fresh water is used as FS), $\Delta P/\Delta\pi_0$ and θ are essentially the same. In such a case, NSEP is solely dependent on γ and θ. The result is shown in Figure 2. Apparently, for any given γ, there is a maximum of NSEP.

To find out the exact solution to θ or $\Delta P/\Delta\pi_0$ corresponding to the maximum of NSEP, an optimization problem is formulated in which Eq. 9 is the objective function and Eq. 7 is a nonlinear equality constraint. To facilitate iterations in

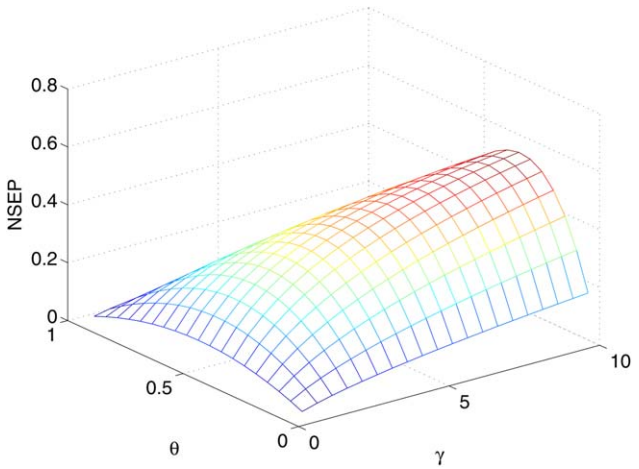

Figure 2. NSEP in PRO as a function of γ and θ. $r = 0$.

[Color figure can be viewed in the online issue, which is available at wileyonlinelibrary.com.]

optimization, a variable $z = \ln[(\alpha-1)/(\alpha-q_d)]$ is introduced, where $\alpha = 1/\theta$. The optimization problem is formulated as follows

$$\max_{\alpha,z} \text{NSEP} = (q_d-1)\left(\frac{1}{\alpha}-r\right)$$
$$\text{s.t.}$$
$$q_d = \alpha-(\alpha-1)e^{-z} \qquad (13)$$
$$\gamma = \alpha(1-q_d+\alpha z)$$
$$1-\alpha \le 0$$
$$1-q_d \le 0$$

which can be solved using optimization packages, for example, fmincon in MATLAB.

The optimal solutions using a wide range of γ values (0.1–100) and representative values of r (0, 0.1, 0.2, and 0.4) are shown in Figure 3. Note that log scale is used in x-axis in these plots. It is seen that when γ is close to 0, $\Delta P_{opt} = \Delta \pi_0/2$ may be considered valid. However, as γ becomes larger, ΔP_{opt} deviates from $\Delta\pi_0/2$. For example, when $\gamma = 4.5$ and $r = 0$, the ΔP_{opt} is only about 40% of $\Delta\pi_0$, and the DS is diluted twice at the outlet of the membrane. It is further verified that $\overline{\Delta\pi}/2 < \Delta P_{opt} < \Delta\pi_0/2$ in all the cases. The fact that ΔP_{opt} also deviates from $\overline{\Delta\pi}/2$ may be explained by the definition of $\overline{\Delta\pi}$

$$AL_p(\overline{\Delta\pi}-\Delta P) = Q_w = Q_0(q_d-1) \qquad (14)$$

or

$$\overline{\Delta\pi} = \Delta P+\pi_0\frac{q_d-1}{\gamma} \qquad (15)$$

When γ is large, the second term on the right hand side of the above equation is relatively small. As a result, $\overline{\Delta\pi}$ strongly depends on ΔP, and $\Delta P_{opt} \neq \overline{\Delta\pi}/2$ in Eq. 3.

The dimensionless driving force in PRO is defined as $\zeta = (\Delta\pi-\Delta P)/\pi_0^D$. It may be calculated as $1-\theta$ at inlet and $1/q_d-\theta$ at outlet. The average driving force is $\bar{\zeta} = (\overline{\Delta\pi}-\Delta P)/\pi_0^D = (q_d-1)/\gamma$ according to Eq. 15. ζ at both inlet and outlet, as well as $\bar{\zeta}$ using $r = 0$ are shown in Figure 4. It is seen that $\bar{\zeta}$ is not a simple arithmetic mean of inlet and outlet values of ζ. Moreover, as γ becomes adequately large, both the driving force at outlet and the average driving force approach 0, implying thermodynamic equilibrium.[22,25] In the ideal case where $\gamma \to \infty$ and $r = 0$, the optimal NSEP and η_{O2H} approach 1, or all the osmotic energy may be converted to hydraulic energy. The corresponding $\Delta P_{opt} \to 0$, indicating that PRO becomes forward osmosis.

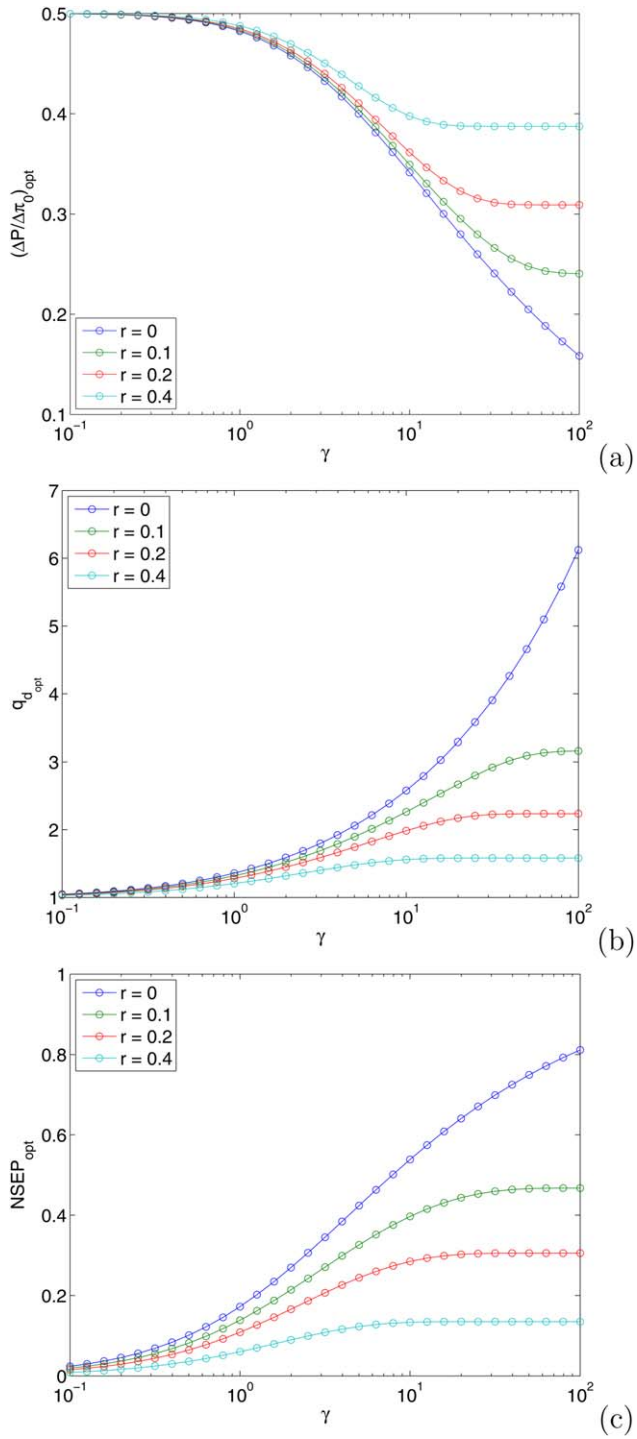

Figure 3. (a) Optimal $\Delta P/\Delta\pi_0$, (b) optimal q_d and (c) optimal NSEP in PRO as a function of γ and r.

[Color figure can be viewed in the online issue, which is available at wileyonlinelibrary.com.]

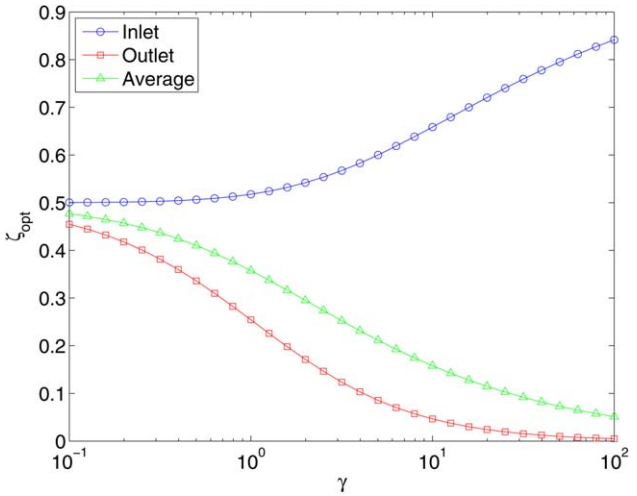

Figure 4. Optimal dimensionless driving forces in PRO as a function of γ. $r = 0$.

[Color figure can be viewed in the online issue, which is available at wileyonlinelibrary.com.]

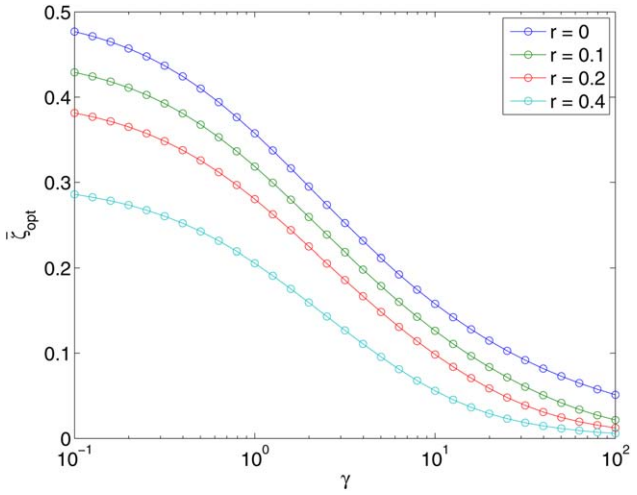

Figure 5. Optimal $\bar{\zeta}$ in PRO as a function of γ and r.

[Color figure can be viewed in the online issue, which is available at wileyonlinelibrary.com.]

The significance of γ is as follows. A larger γ allows the PRO to be operated closer to its thermodynamic limit, thus improving NSEP. This conclusion is very similar to RO in which a larger γ enables the process to be operated near its thermodynamic limit to reduce NSEC (normalized SEC).[22,23,26] However, there is always a trade-off between capital investment and energy production in PRO or energy consumption in RO, thus limiting the magnitude of γ. Based on the author's analysis of numerous industrial-scale plants, γ is about 0.6–0.9 in seawater RO (SWRO).[27] If one uses brine from an industrial SWRO and fresh water for power generation with similar membranes and process conditions, γ in PRO is about 2.4–3.6 (because salinity is doubled and flow is halved when evaluating γ, based on a typical recovery of 50% in SWRO). It is shown that η_{O2H} is about 30–37%. For a PRO system using ocean water and fresh water, γ is reduced to 1.2–1.8, and η_{O2H} is 20–25%. Note that these do not account for the effect of concentration polarization (a more severe effect in PRO than in RO[14]) which will be discussed later.

The average driving force $\bar{\zeta}$ using different values of r is shown in Figure 5. From Figures 3 and 5, one may conclude that an increase in FS salinity reduces driving force for water flow, leading to a decrease in DS dilution ratio and power production. At $\gamma = 4.5$, an increase in r from 0 to 0.1 results in a significant 23% reduction in η_{H2O} (from 41 to 31%). This change is attributed to a 9% reduction in ΔP and a 15% reduction in Q_w in Eq. 3.

From the relationship between NSEP and γ in Figure 3, one may derive the effect of membrane area A, permeability L_p, DS inlet flow Q_0 and inlet transmembrane osmotic pressure $\Delta\pi_0$ on η_{O2H} and PD, using equivalent relationships shown in Table 1. The results based on $r = 0$ are shown in Figure 6. Standard linear scales are used. It is noted that all the relationships (except for $\Delta\pi_0$ vs. PD) are very nonlinear in a wide range. Moreover, a smaller membrane tends to have a higher PD if the other three parameters are the same.

Analysis accounting for concentration polarization

As mentioned earlier, PRO is severely affected by concentration polarization, which reduces water flux and power generation.[28] In the presence of both internal concentration polarization (ICP) and external concentration polarization (ECP), the water flux in PRO is described by[9,11]

$$J_w = L_p\left[\pi_b^D \exp\left(-\frac{J_w}{k_m}\right)\frac{1-\frac{\pi_b^F}{\pi_b^D}\exp\left(J_w K\right)\exp\left(\frac{J_w}{k_m}\right)}{1+\frac{B}{J_w}\left[\exp\left(J_w K\right)-1\right]}-\Delta P\right] \tag{16}$$

where k_m is mass-transfer coefficient, K is solute resistivity, B is solute permeability coefficient, and subscript b represents bulk property. When k_m is adequately large and K is sufficiently small, Eq. 16 reduces to Eq. 1. In the presence of concentration polarization, the hydraulic power is $W = Q_w \Delta P = \Delta P \int_0^A J_w dA$, the same as before.

The flux in Eq. 16 is in an implicit form and can only be solved numerically. However, with some simplifications, an explicit solution may be possible, and the conclusions in the previous subsection become relevant.

If $J_w/k_m \ll 1$[9] and $J_w K \ll 1$,[14] the following approximations may be made: $\exp\left(J_w K\right) = 1 + J_w K$ and $\exp\left(J_w/k_m\right) = 1 + J_w/k_m$. As a result, Eq. 16 is simplified as

$$\begin{aligned} J_w &\approx L_p\left[\pi_b^D\left(1-\frac{J_w}{k_m}\right)\frac{1-\frac{\pi_b^F}{\pi_b^D}\left(1+J_w K\right)\left(1+\frac{J_w}{k_m}\right)}{1+BK}-\Delta P\right] \\ &= L_p\left[\left(1-\frac{J_w}{k_m}\right)\frac{\pi_b^D-\pi_b^F\left(1+J_w K\right)\left(1+\frac{J_w}{k_m}\right)}{1+BK}-\Delta P\right] \\ &\approx L_p\left[\left(1-\frac{J_w}{k_m}\right)\frac{\pi_b^D-\pi_b^F}{1+BK}-\Delta P\right] \\ &= L_p\left[\left(1-\frac{J_w}{k_m}\right)\frac{\Delta\pi}{1+BK}-\Delta P\right] \end{aligned} \tag{17}$$

or

$$J_w = L_p'\left(\sigma\Delta\pi-\Delta P\right) \tag{18}$$

Table 1. Effect of Process Parameters on Power Efficiency and Density Based on γ vs. NSEP

Relationship	Equivalent relationship
A (or L_p or $\Delta\pi_0$) vs. η_{O2H}, or L_p vs. PD	γ vs. NSEP
Q_0 vs. η_{O2H}	$1/\gamma$ vs. NSEP
$\Delta\pi_0$ vs. PD	γ vs. NSEPγ
Q_0 vs. PD	$1/\gamma$ vs. NSEP$/\gamma$
A vs. PD	γ vs. NSEP$/\gamma$

where $\sigma = 1/(1+BK)$ and $L'_p = L_p/(1+L_p\Delta\pi\sigma/k_m)$. In this sense, the significance of concentration polarization is that it reduces the effective transmembrane osmotic pressure ($\Delta\pi_{eff} = \sigma\Delta\pi < \Delta\pi$) and hydraulic permeability ($L'_p < L_p$).

When $\Delta\pi$ may be considered as constant (e.g., $\gamma \to 0$), an approximate analytical solution to the optimal ΔP is as follows

$$\Delta P_{opt} = \frac{\sigma}{2}\Delta\pi \tag{19}$$

The maximum power of PRO assuming constant $\Delta\pi$ may be calculated by

$$W_{opt} = \frac{1}{2}\sigma\Delta\pi J'_w A \tag{20}$$

where J'_w is the flux that satisfies Eq. 16 when $\Delta P = \sigma\Delta\pi/2$. Some iterations are required to solve J'_w, but Eq. 20 is more accurate than $AL'_p\sigma^2(\Delta\pi)^2/4$. The difference between both methods is a few percent.

If the effect of ECP is negligible (e.g., streams on both sides of the membrane are stirred to suppress boundary layer development), Eq. 16 is simplified as

$$J_w = L_p(\sigma\Delta\pi - \Delta P) \tag{21}$$

In such a case, Eq. 7 should be replaced by

$$\gamma = \frac{1}{\theta}\left[(1-q_d) + \frac{\sigma}{\theta}\ln\frac{\sigma-\theta}{\sigma-q_d\theta}\right] \tag{22}$$

to describe the coupled phenomena in PRO. When ECP is small but not negligible, Eq. 22 may still be used if γ is replaced by γ' ($\gamma' = AL'_p\pi_0^D/Q_0$).

The maximization of NSEP accounting for concentration polarization may be determined by solving the following optimization problem

$$\begin{aligned} &\max_{\alpha,z} \text{NSEP} = (q_d-1)\left(\frac{1}{\alpha}-r\right) \\ &s.t. \\ &q_d = \alpha\sigma - (\alpha\sigma-1)e^{-z} \\ &\gamma = \alpha(1-q_d+\alpha\sigma z) \\ &1/\sigma - \alpha \le 0 \\ &1-q_d \le 0 \end{aligned} \tag{23}$$

Equation 23 is solved using $\sigma = 0.9$ and $r = 0$, and the results are shown in Figure 7. The results without ICP (i.e., $\sigma = 1$) are also provided for a comparison. Based on these approximate solutions, it is seen clearly that ICP reduces the magnitude of the optimal ΔP that should be applied in PRO. Moreover, water across the membrane is smaller. As a result, the power generation is lower.

It is observed that as $\gamma \to 0$, the following relationships hold

$$\begin{aligned} \frac{\theta_{opt,ICP}}{\theta_{opt,ideal}} &= \sigma \\ \frac{q_{d_{opt,ICP}}-1}{q_{d_{opt,ideal}}-1} &= \sigma \\ \frac{\text{NSEP}_{opt,ICP}}{\text{NSEP}_{opt,ideal}} &= \sigma^2 \\ \frac{\bar{\zeta}_{opt,ICP}}{\bar{\zeta}_{opt,ideal}} &= \sigma \end{aligned} \tag{24}$$

To provide the exact solution (i.e., without assuming $J_w/k_m \ll 1$ or $J_wK \ll 1$) to water flow and power generation in PRO where $\Delta\pi$ is changing along the membrane, the following equation

$$\frac{dQ}{dx} = AJ_w, Q = Q_0 \quad @x = 0$$

$$J_w = L_p\left[\pi_b^D \exp\left(-\frac{J_w}{k_m}\right)\frac{1-\frac{\pi_b^F}{\pi_b^D}\exp(J_wK)\exp\left(\frac{J_w}{k_m}\right)}{1+\frac{B}{J_w}[\exp(J_wK)-1]} - \Delta P\right] \tag{25}$$

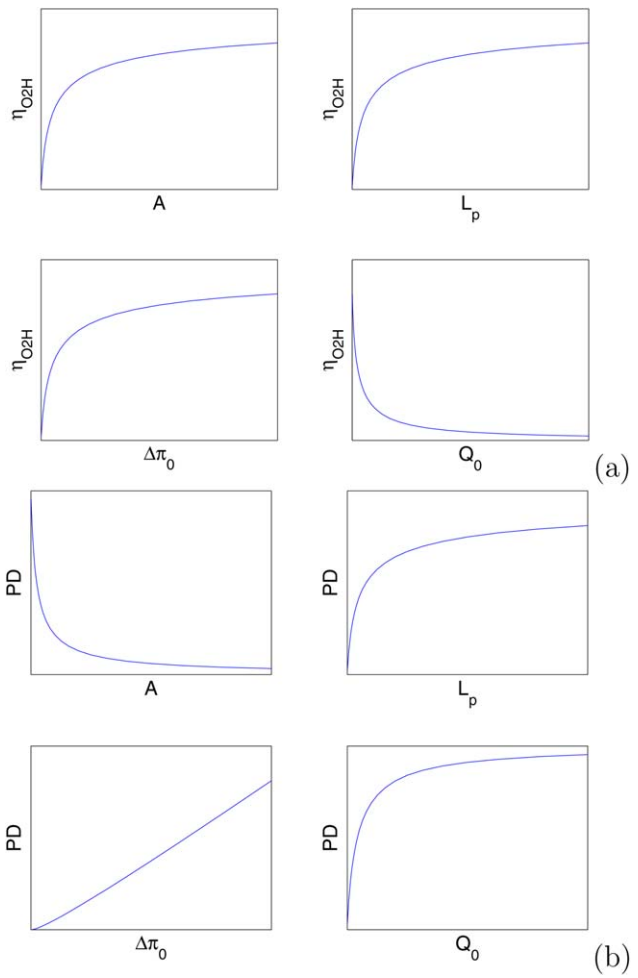

Figure 6. Effect of A, L_p, Q_0, $\Delta\pi_0$ on (a) energy conversion efficiency and (b) power density in PRO under optimal conditions. $r = 0$.

[Color figure can be viewed in the online issue, which is available at wileyonlinelibrary.com.]

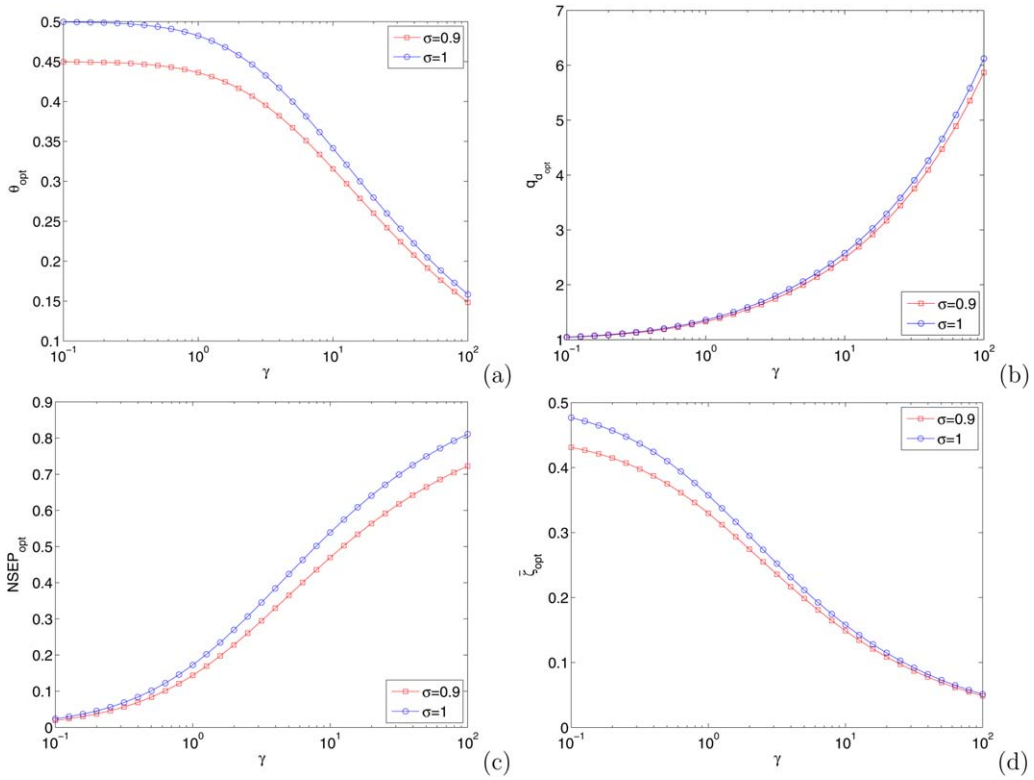

Figure 7. Effect of ICP on (a) optimal θ, (b) optimal q_d, (c) optimal NSEP, and (d) optimal average driving force. $r = 0$.

[Color figure can be viewed in the online issue, which is available at wileyonlinelibrary.com.]

has to be integrated numerically from the inlet to the outlet of the membrane. The procedure is as follows:

1. With given parameters B, K, k_m, L_p, ΔP and π_b^D, π_b^F, solve local J_w numerically at membrane position x using Eq. 22.

2. Integrate Eq. 25 for one step from x to $x+\Delta x$. Update Q.

3. Update π_b^D and π_b^F, that is, $\pi_b^D = \pi_0^D Q_0/Q, \pi_b^F = \pi_0^F Q_0^F/(Q_0^F+Q_0-Q)$. Note that no salt leakage is assumed here.

4. Repeat steps 2–3 until reaching the end of the membrane, or x = 1. The DS flow at outlet is recorded as Q_1. $Q_w = Q_1 - Q_0$.

5. Calculate $PD = Q_w \Delta P/A$.

The following steps may be used to find the maximum of PD and ΔP_{opt}:

6. Repeat steps 1–5 using different values of ΔP.

7. Sort the PDs. Find the highest PD and the corresponding ΔP_{opt}.

It is worth noting that steps 6–7 may be replaced by optimization algorithms (e.g., Quasi-Newton, BFGS), however, iterative executions of steps 1–5 are still required to find the maximum of PD. The steps 1–7 are used in this work because it is possible to show the general trend of PD in a wide range of ΔP.

The parameters used for optimization are shown in Table 2. These parameters are taken from a recent literature[9] which are assumed to represent properties of currently available membranes. Two concentrations of 35 g/L (similar to concentration of seawater) and 60 g/L NaCl (similar to concentration of SWRO brine) are used for the DS and fresh water is used for the FS. When $\Delta\pi$ is changing along the membrane, the effect of dilution in the DS on PRO performance is investigated by varying Q_0/A values (1×10^{-6}, 2×10^{-6}, 4×10^{-6}, and 8×10^{-6} m/s).

Both rigorous and short-cut solution methods are used for a comparison. The rigorous solution methods refer to those based on $PD = J_w \Delta P$ (where J_w is calculated by Eq. 16) when $\Delta\pi$ is constant (i.e., $\gamma \to 0$) or $PD = \Delta P \int_0^A J_w dA/A = Q_w \Delta P/A$ (where Q_w is based on Eq. 25) when $\Delta\pi$ is changing along the membrane (i.e., γ is finite). A wide range of ΔP with an interval of 10 kPa are tried, and the results are sorted to find the maximum of PD and the corresponding ΔP_{opt}. The approximate short-cut solution methods solve the ΔP_{opt} directly using Eq. 19 when $\Delta\pi$ is constant or Eq. 23 when $\Delta\pi$ is changing along the membrane. After ΔP_{opt} is determined, J_w is calculated based on Eq. 16 when $\Delta\pi$ is constant, or Q_w is calculated based on Eq. 25 when $\Delta\pi$ is changing. The maximum of PD is determined accordingly.

The results are summarized in Table 3 and Figure 8. In all cases, the short-cut solution methods yield essentially the same maximum PD without tedious procedures required by the rigorous solution methods. Moreover, using the short-cut methods, the shift of ΔP_{opt} due to concentration polarization

Table 2. Parameters Used in the Simulation of PRO[9]

Parameters	Value
k_m	8.48×10^{-5} m/s
K	4.51×10^{5} s/m
B	1.11×10^{-7} m/s
L_p	1.87×10^{-9} m/s/kPa
$\Delta\pi_0$	2763, 4882 kPa

Table 3. Optimization Results of Power Density and Efficiency

$\Delta\pi_0$=2763 kPa	ΔP_{opt}, kPa	$\overline{J_{w\,opt}}$, 10^{-6} m/s	PD_{opt}, W/m^2	γ	$q_{d_{opt}}$	$\eta_{O2H_{opt}}$, %
$\Delta\pi=\Delta\pi_0$	1330 (1316)	2.16 (2.18)	2.87	–	–	–
$Q_0/A=8\times10^{-6}$ m/s	1300 (1295)	1.78 (1.79)	2.31	0.65	1.22	10.5
$Q_0/A=4\times10^{-6}$ m/s	1260 (1259)	1.56 (1.56)	1.96	1.29	1.39	17.7
$Q_0/A=2\times10^{-6}$ m/s	1190 (1186)	1.28 (1.28)	1.52	2.58	1.64	27.6
$Q_0/A=1\times10^{-6}$ m/s	1070 (1067)	1.00 (1.01)	1.07	5.17	2.01	38.9
$\Delta\pi_0$=4882 kPa						
$\Delta\pi=\Delta\pi_0$	2390 (2325)	3.38 (3.47)	8.07	–	–	–
$Q_0/A=8\times10^{-6}$ m/s	2260 (2244)	2.64 (2.66)	5.97	1.14	1.33	15.3
$Q_0/A=4\times10^{-6}$ m/s	2140 (2133)	2.24 (2.25)	4.79	2.28	1.56	24.6
$Q_0/A=2\times10^{-6}$ m/s	1950 (1943)	1.79 (1.80)	3.50	4.56	1.90	35.8
$Q_0/A=1\times10^{-6}$ m/s	1680 (1685)	1.38 (1.38)	2.32	9.13	2.37	47.4

and dilution is clearly revealed. Very minor differences in ΔP_{opt} and average water flux $\overline{J_{w\,opt}}$ are observed (those obtained using short-cut methods are presented in parenthesis).

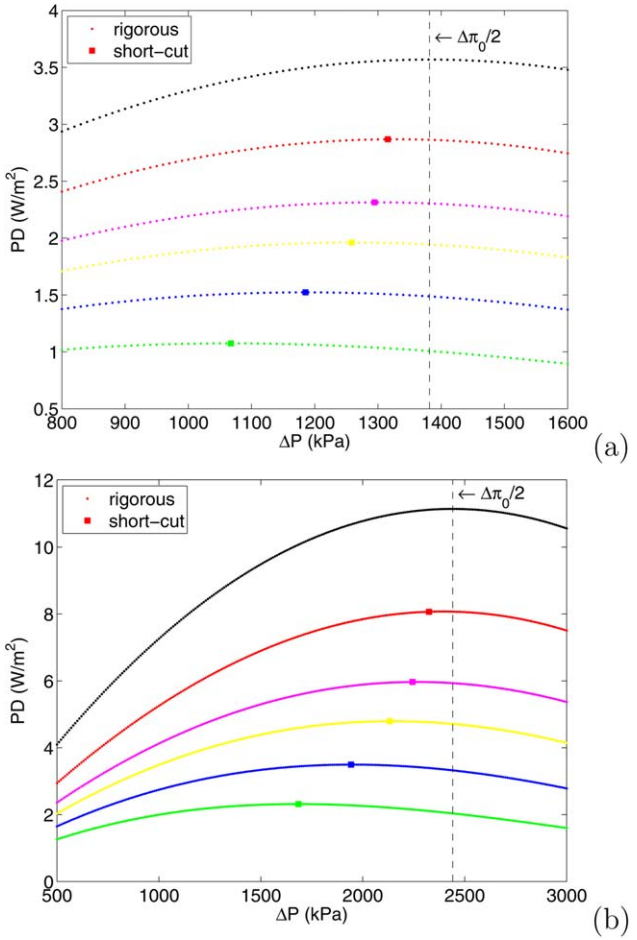

Figure 8. Comparison between rigorous and approximate short-cut solutions of optimal conditions in PRO for (a) $\Delta\pi_0=2763$ kPa, (b) $\Delta\pi_0=4882$ kPa.

Black symbols: theoretical calculation of PD by $L_p\Delta P(\Delta\pi_0-\Delta P)$. Red symbols: $\Delta\pi=\Delta\pi_0$ and concentration polarization is considered. Magenta symbols: $Q_0/A=8\times10^{-6}$ m/s. Yellow symbols: $Q_0/A=4\times10^{-6}$ m/s. Blue symbols: $Q_0/A=2\times10^{-6}$ m/s. Green symbols: $Q_0/A=1\times10^{-6}$ m/s. [Color figure can be viewed in the online issue, which is available at wileyonlinelibrary.com.]

The effect of concentration polarization is shown by the difference between the black and red dotted lines. Even if there is no dilution in DS (i.e., $\Delta\pi=\Delta\pi_0$), there is a slight shift of ΔP_{opt} from $\Delta\pi_0/2$ in both DS concentrations. This may be explained by Eq. 19 ($\sigma=0.95$ based on parameters in Table 2). Because of additional mass-transfer resistance induced by concentration polarization, the flux is smaller. Under optimal PD conditions, the flux reduces from 2.58×10^{-6} m/s to 2.16×10^{-6} m/s when $\Delta\pi_0=2763$ kPa and from 4.56×10^{-6} m/s to 3.38×10^{-6} m/s when $\Delta\pi_0=4882$ kPa. Concentration polarization leads to 20 and 28% reductions in PD in these two cases.

The effect of dilution in DS is demonstrated by the difference between red and four other colored (magenta, yellow, blue and green) dotted lines. As one example, at $Q_0/A=2\times10^{-6}$ m/s, the ΔP_{opt} is only 43% of $\Delta\pi_0$ when $\Delta\pi_0=2763$ kPa and 40% when $\Delta\pi_0=4882$ kPa, because of the γ effect explained earlier. The $q_{d_{opt}}$ are 1.64 and 1.90, respectively, implying that there is a significant dilution in DS at the end of the membrane. The dilution in DS leads to 47 and 57% reductions in PD as compared to the cases without dilution (i.e., $\Delta\pi=\Delta\pi_0$). It is worth pointing out that $\Delta P_{opt}<\Delta\pi_0/2$ is supported by several experimental observations reported in literature.[11,13,29]

As γ increases, $q_{d_{opt}}$ increases and ΔP_{opt} decreases. As a result, $\overline{J_{w\,opt}}$ decreases. Profiles of J_w along the membrane channel are shown in Figure 9. As expected, when DS is diluted, J_w reduces longitudinally.

In each individual case in Table 3, maximizing NSEP (or η_{O2H}) and maximizing PD are equivalent because Q/A_0, L_p and π_0^D are fixed (see Eq. 11). However, if one looks at the data globally, power density and efficiency follow opposite trends, that is, as γ increases, η_{O2H} increases but PD decreases. In the author's opinion, PD focuses on membrane cost while NSEP (or η_{O2H}) considers pumping (note that the pressure drop in feed channels are ignored in this work), pre- and post-treatment costs in PRO. A trade-off is necessary to minimize total cost in PRO since these two factors are conflicting. For instance, if $Q_0/A=2\times10^{-6}$ m/s is chosen ($\gamma=2.58$ for $\Delta\pi_0=2763$ kPa and 4.56 for $\Delta\pi_0=4882$ kPa, slightly higher than industrial SWRO conditions), η_{O2H} is estimated to be 28 and 36% using seawater and brine of SWRO as DS and fresh water as FS. The corresponding PDs are approximately 1.5 and 3.5 W/m^2.

Note that the aforementioned trends are based on fixed membrane properties. If the hydraulic permeability L_p is boosted and all the other parameters remain the same, both PD and η_{O2H} will be enhanced, as suggested by Figure 6. For example, in the case of $Q_0/A=4\times10^{-6}$ m/s and $\Delta\pi_0=$

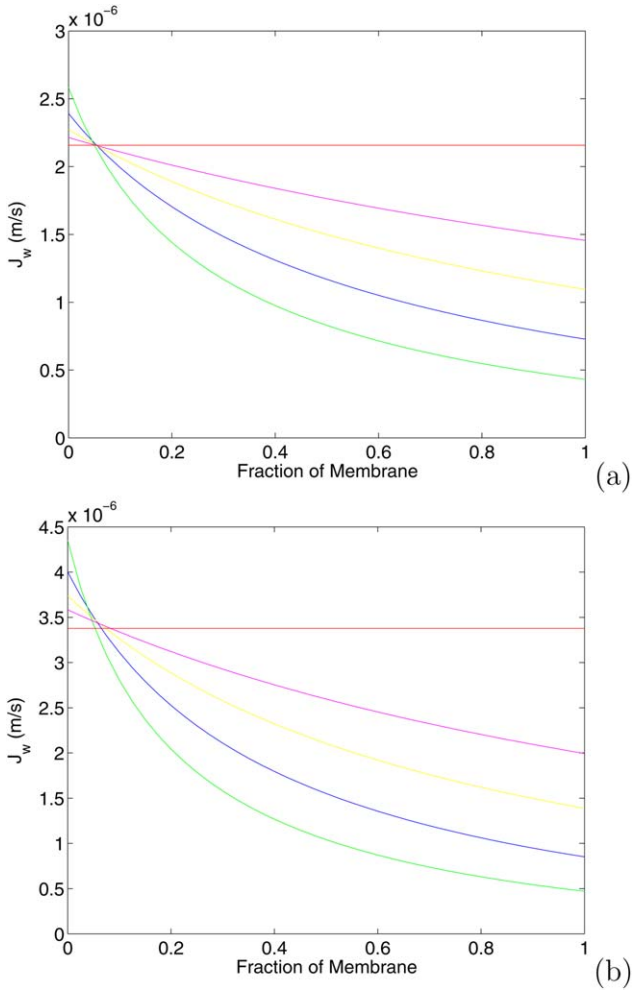

Figure 9. Profiles of flux under optimal conditions in PRO for (a) $\Delta\pi_0$=2763 kPa and (b) $\Delta\pi_0$=4882 kPa.

Red: $\Delta\pi=\Delta\pi_0$ and concentration polarization is considered. Magenta: $Q_0/A=8\times10^{-6}$ m/s. Yellow: $Q_0/A=4\times10^{-6}$ m/s. Blue: $Q_0/A=2\times10^{-6}$ m/s. Green symbols: $Q_0/A=1\times10^{-6}$ m/s. [Color figure can be viewed in the online issue, which is available at wileyonlinelibrary.com.]

2763 kPa, if L_p is doubled, optimization calculation shows that η_{O2H} increases from 17.7 to 26.1% (close to 27.6%, the η_{O2H} in the case of $Q_0/A=2\times10^{-6}$ m/s in Table 3. They have the same magnitude of γ. However, the effect of concentration polarization is slightly different), and PD increases from 1.96 to 2.89 W/m^2 (close to twice of 1.52 W/m^2, the PD in the case of $Q_0/A=2\times10^{-6}$ m/s in Table 3. The difference is due to different effects of concentration polarization).

In the operation of membrane processes, membrane properties may degrade slowly with respective to time, and L_p reduces.[30] Based on the above discussions, the best applied pressure ΔP_{opt} may gradually shift toward $\Delta\pi_0/2$ during operation of PRO as L_p decreases. The maximum of PD would reduce.

Besides hydraulic permeability, improving other membrane properties would be beneficial for water flux. For example, it is reported that modifying membrane structures[31] suppresses ICP, and improving hydrodynamics in membrane feed channels reduces ECP.[12] Such research and development efforts complement system-level optimization, and are indispensable to enhance the economics of PRO.

Conclusions

In addition to concentration polarization discussed extensively in literature, the performance of PRO is also severely affected by dilution in DS along the membrane channel. A dimensionless parameter γ, originally developed in analysis and optimization of RO processes, is used to quantify this phenomenon. Because of these two factors, the best applied pressure in PRO operation shifts lower than $\Delta\pi_0/2$ and the power density may be significantly reduced.

With fixed membrane properties, power density and osmotic to hydraulic efficiency follow opposite trends as operating conditions change. As the dilution effect appears inevitable, improving membrane properties (hydraulic permeability and mass-transfer characteristics) is crucial to enhance the economic feasibility of PRO.

Acknowledgment

Office of Faculty Affairs at California State Polytechnic University, Pomona is acknowledged for sponsoring Mingheng Li's sabbatical leave during which part of this work was conducted.

Notations

Acronyms

DS = Draw solution
ECP = External concentration polarization
FS = Feed solution
ICP = Internal concentration polarization
NSEC = Normalized specific energy consumption
NSEP = Normalized specific energy production
PD = Power density
PRO = Pressure retarded osmosis
RO = Reverse osmosis
SEC = Specific energy consumption
SEP = Specific energy production
SWRO = Seawater reverse osmosis

Greek symbols

α = $\pi_0^D/(\Delta P+\pi_0^F)$, -
ΔP = Transmembrane hydraulic pressure difference, kPa
$\Delta\pi$ = Transmembrane osmotic pressure difference, kPa
$\Delta\pi_{eff}$ = Effective transmembrane osmotic pressure difference, kPa
η_{O2H} = Osmotic energy to hydraulic energy efficiency in PRO, -
γ = $AL_p\pi_0^D/Q_0$, -
π = Osmotic pressure, kPa
σ = $1/(1+BK)$, -
θ = $(\Delta P+\pi_0^F)/\pi_0^D$, -
ζ = Driving force divided by π_0^D, -

Roman symbols

A = Membrane area, m^2
B = Salt permeability coefficient, m/s
J_w = Water flux across membrane, m/s
K = Solute resistivity, s/m
k_m = Mass transfer coefficient, m/s
L_p = Hydraulic permeability, m/s/kPa
P = pressure, kPa
Q = Draw solution flow rate, m^3/s
q = Q/Q_0, -
Q^F = Feed solution flow rate, m^3/s
q_d = Dilution ratio of DS, -
Q_w = Water flow across membrane, m^3/s

r = Osmotic pressure ratio π_0^F/π_0^D, -
W = Power generated by PRO, kW

Superscripts

^{D} = Draw solution property
^{F} = Feed solution property

Subscripts

$_0$ = Inlet property
$_b$ = Bulk property
$_{opt}$ = Optimal solution

Literature Cited

1. Loeb S, Norman RS. Osmotic power plants. *Science*. 1975;189:654–655.
2. Kim YC, Elimelech M. Potential of osmotic power generation by pressure retarded osmosis using seawater as feed solution: analysis and experiments. *J Membr Sci*. 2013;429:330–337.
3. Loeb S. Large-scale power production by pressure-retarded osmosis, using river water and sea water passing through spiral modules. *Desalination*. 2002;143:115–122.
4. Helfer F, Lemckert C, Anissimov YG. Osmotic power with pressure retarded osmosis: theory, performance and trends—A review. *J Membr Sci*. 2014;453:337–358.
5. Achilli A, Childress AE. Pressure retarded osmosis: from the vision of Sidney Loeb to the first prototype installation—Review. *Desalination*. 2010;261:205–211.
6. Logan BE, Elimelech M. Membrane-based processes for sustainable power generation using water. *Nature*. 2012;488:313–319.
7. Skilhagen SE, Dugstad JE, Aaberg RJ. Osmotic power—power production based on the osmotic pressure difference between waters with varying salt gradients. *Desalination*. 2008;220:476–482.
8. Thorsen T, Holt T. The potential for power production from salinity gradients by pressure retarded osmosis. *J Membr Sci*. 2009;335:103–110.
9. Achilli A, Cath TY, Childress AE. Power generation with pressure retarded osmosis: an experimental and theoretical investigation. *J Membr Sci*. 2009;343:42–52.
10. Saito K, Irie M, Zaitsu S, Sakai H, Hayashi H, Tanioka A. Power generation with salinity gradient by pressure retarded osmosis using concentrated brine from SWRO system and treated sewage as pure water. *Desalin Water Treat*. 2012;41:114–121.
11. Xu Y, Peng X, Tang CY, Fu QS, Nie S. Effect of draw solution concentration and operating conditions on forward osmosis and pressure retarded osmosis performance in a spiral wound module. *J Membr Sci*. 2010;348:298–309.
12. Yip NY, Elimelech M. Performance limiting effects in power generation from salinity gradients by pressure retarded osmosis. *Environ Sci Technol*. 2011;45:10273–10282.
13. She Q, Jin X, Tang CY. Osmotic power production from salinity gradient resource by pressure retarded osmosis: effects of operating conditions and reverse solute diffusion. *J Membr Sci*. 2012;401–402:262–273.
14. Lee KL, Baker RW, Lonsdale HK. Membranes for power generation by pressure-retarded osmosis. *J Membr Sci*. 1981;8:141–171.
15. Sharqawy MH, Banchik LD, Lienhard JH. Effectiveness-mass transfer units (ε-MTU) model of an ideal pressure retarded osmosis membrane mass exchanger. *J Membr Sci*. 2013;445:211–219.
16. Sivertsen E, Holt T, Thelin W, Brekke G. Modelling mass transport in hollow fibre membranes used for pressure retarded osmosis. *J Membr Sci*. 2012;417–418:69–79.
17. Tan CH, Ng HY. Modified models to predict flux behavior in forward osmosis in consideration of external and internal concentration polarizations. *J Membr Sci*. 2008;324:209–219.
18. Yip NY, Elimelech M. Thermodynamic and energy efficiency analysis of power generation from natural salinity gradients by pressure retarded osmosis. *Environ Sci Technol*. 2012;46:5230–5239.
19. Sharqawy MH, Zubair SM, Lienhard JH. Second law analysis of reverse osmosis desalination plants: an alternative design using pressure retarded osmosis. *Energy*. 2011;36:6617–6626.
20. Kim YC, Kim Y, Oh D, Lee KH. Experimental investigation of a spiral-wound pressure-retarded osmosis membrane module for osmotic power generation. *Environ Sci Technol*. 2013;47:2966–2973.
21. Sagiv A, Zhu A, Christofides PD, Cohen Y, Semiat R. Analysis of forward osmosis desalination via two-dimensional FEM model. *J Membr Sci*. 2014;464:161–172.
22. Li M. Minimization of energy in reverse osmosis water desalination using constrained nonlinear optimization. *Ind Eng Chem Res*. 2010;49:1822–1831.
23. Li M. Reducing specific energy consumption in reverse osmosis (RO) water desalination: an analysis from first principles. *Desalination*. 2011;276:128–135.
24. Post JW, Veerman J, Hamelers HVM, Euverink GJW, Metz SJ, Nymeijer K, Buisman CJN. Salinity-gradient power: Evaluation of pressure-retarded osmosis and reverse electrodialysis. *J Membr Sci*. 2007;288:218–230.
25. Zhu A, Christofides PD, Cohen Y. Effect of thermodynamic restriction on energy cost optimization of RO membrane water desalination. *Ind Eng Chem Res*. 2009;48:6010–6021.
26. Li M. Energy consumption in spiral-wound seawater reverse osmosis at the thermodynamic limit. *Ind Eng Chem Res*. 2014;53:3293–3299.
27. Li M. A unified model-based analysis and optimization of specific energy consumption in BWRO and SWRO. *Ind Eng Chem Res*. 2013;52:17241–17248.
28. Mccutcheon JR, Elimelech M. Modeling water flux in forward osmosis: implications for improved membrane design. *AIChE J*. 2007;53:1736–1744.
29. Sharif AO, Merdaw AA, Aryafar M, Nicoll P. Theoretical and experimental investigations of the potential of osmotic energy for power production. *Membranes*. 2014;4:447–468.
30. Li M. Optimization of multitrain brackish water reverse osmosis (BWRO) desalination. *Ind Eng Chem Res*. 2012;51:3732–3739.
31. Wang KY, Ong RC, Chung TS. Double-skinned forward osmosis membranes for reducing internal concentration polarization within the porous sublayer. *Ind Eng Chem Res*. 2010;49:4824–4831.

Manuscript received Nov. 2, 2014, and revision received Dec. 10, 2014.